# Cu(I) and Ag(I) Complexes of 7,10-bis-N-heterocycle-diazafluoranthenes: Programmed Molecular Grids?

**Nelli Rahanyan, Simon Duttwyler, Anthony Linden, Kim K. Baldridge and Jay S. Siegel***

*Institute of Organic Chemistry, University of Zürich, Winterthurerstrasse 190, 8057 Zürich, Switzerland*



Reactions of 7,10-disubstituted diazafluoranthene derivatives with three different silver(I) salts AgX (X = $[PF_6]^-$, $[SbF_6]^-$, $[CB_{11}HCl_{11}]^-$) and $[Cu(CH_3CN)_4]PF_6$ afforded complexes exhibiting five different motifs. The crystal structures of the free ligands and nine new complexes from this series of reactions are reported. The use of 2,5-di-*tert*-butyl-7,10-di(pyridin-2-yl)-8,9-diazafluoranthene as a ligand leads to the formation of the tetranuclear compounds $[Ag_4(C_{32}H_{30}N_4)_4][PF_6]_4\cdot 3C_6H_6\cdot 4MeCN$, $[Ag_4(C_{32}H_{30}N_4)_4][SbF_6]_4\cdot 4C_5H_{12}$ and $[Cu_4(C_{32}H_{30}N_4)_4][PF_6]_4\cdot 8C_3H_6O$, which exhibit "propeller" and saddle-type geometry, respectively, as well as a dinuclear complex $[Ag_2(C_{32}H_{30}N_4)_2][CHB_{11}Cl_{11}]_2\cdot 4C_6H_4Cl_2\cdot CH_2Cl_2$. The reactions involving the less sterically hindered 2,5-di-*tert*-butyl-7,10-di-(pyrimidin-2-yl)-8,9-diazafluoranthene and 2,5-di-*tert*-butyl-7,10-di(thiazol-2-yl)-8,9-diazafluoranthene afforded crystals of the dinuclear complexes $[Ag_2(C_{30}H_{28}N_6)_2][PF_6]_2\cdot 0.5CH_2Cl_2\cdot 0.5C_6H_5Cl\cdot 4C_6H_{14}$, $[Ag_2(C_{30}H_{28}N_6)_2][SbF_6]_2\cdot C_3H_6O\cdot 0.5C_6H_{14}\cdot 0.5C_6H_6$, the polymeric species $[Ag_2(C_{28}H_{26}N_4S_2)_2]_n\oplus 2n[PF_6]_n\cdot nC_3H_6O$ and the tetranuclear compounds $[Cu_4(C_{26}H_{25}N_4S_2)_4][PF_6]_4\cdot 2CHCl_3\cdot C_3H_6O$ and $[Cu_4(C_{30}H_{28}N_6)_4][PF_6]_4\cdot 2.17H_2O$, which possess saddle and grid-like architectures, respectively. Conformational analysis of the free ligands showed that they exhibit N–C–C–N torsion angles ranging from *syn clinal* (58°) to fully *anti-periplanar* conformations; the *syn clinal* conformation dominates in the complexes. The relative energies of the possible structural conformations of the synthesized ligands as well as an oxazol disubstituted diazafluoranthenes was carried out using density functional theory at the B97D/Def2TZVPP level of theory.

## Introduction

Transition metal coordination chemistry provides a powerful methodology for the construction of various metallosupramolecular architectures, which are of interest in the fields of chemistry and biology.[1-3] The taxonomy of such assemblies comprises helicates,[2,4] cages,[5] rotaxanes6 and grids.[7,8] Grid-like complexes are of particular interest due to their physicochemical and electronic properties.[9,10] Schematic representation of the formation of [2x2] grids is illustrated in Fig. 1.

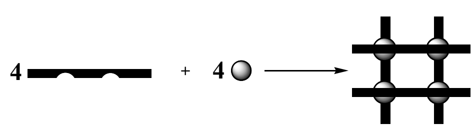

**Fig. 1** Construction of [2x2] grid-type metalloarray $[M_4(L)_4]^{4+}$

The construction of coordination grids based on dipyridylpyrazine and Cu(I) or Ag(I) has been used to support the hypothesis that supramolecular assembly can be programmed at the molecular level with engineering or simple algorithmic robustness;[11-14] however, in supramolecular chemistry small imbalances of energy often cause major structure/property changes that may "surprise" the molecular engineer. The present study probes this hypothesis for a simple array of related ligands (7,10-disubstituted-8,9-diazafluoranthene derivatives **1-3**), "tetrahedral" metals ($Cu^+$, $Ag^+$) and counterions (X = $[PF_6]^-$, $[SbF_6]^-$, $[CB_{11}HCl_{11}]^-$). Analysis of the resultant crystalline structures in light of ligand-field strength, ligand conformational preference, and counter ion participation, indicates that neither the geometry nor robustsness of these structures supports the oversimplified analysis of the "programmable" synthesis hypothesis.

**Ligand design**. A *syn-periplanar* arrangement of nitrogen atom lone pairs in fluoranthene derivatives defines the "ideal" conformation for the assembly of a [2×2] molecular grid comprising bis-bidentate ligands and tetrahedral metals. Even the simplest dipyridylpyrazine prefers the *anti-periplanar* form; so formation of the grid must come at some conformational rearrangment energy cost. The modular syntheses of diazafluoranthene derivatives **1-3** by [2 + 4] cycloaddition reactions of 4,7-di-*tert*-butylacenaphthy-lene and 3,6-disubstituted 1,2,4,5-tetrazines,[15] allows the study of a closely related set of ligands with variable conformational preferences and variable enegry costs associated with the syn periplanar arrangement (Fig. 2). In the case of compound **1**, steric repulsion between hydrogen atoms in the adjacent pyridyl and acenaphthylene rings would force the pyridyl ring out of the pyridazine plane, leading to α > 0°. Lesser steric *H*–heterocycle interactions in **2** and **3** reduce syn periplanar costs; but, does the energy balance tip in favor of the [2x2] molecular grid in a readily foreseeable way? The systematic study of this metal-ligand array provides a context for answering this question.

## Results and discussion

Mixing equimolar amounts of a ligand (**1**-**3**) and a Cu[X] or Ag[X] salt (X = $[PF_6]^-$, $[SbF_6]^-$, $[CB_{11}HCl_{11}]^-$) gave homogeneous solutions in acetone, acetonitrile, dichloromethane or nitromethane, which displayed a single set of $^1$H NMR signals consistent with metal interactions at the nitrogen atoms of the ligands. The solutions also showed UV-vis absorptions consistent with nitrogen-metal complexation.

**Mass spectrometry data.** ESI MS data from solutions of **1** with Cu(I) salts exhibited *m/z* ion signals indictative of $[Cu(\mathbf{1})_3\text{+H}]^+$ (1476.4), $[Cu_2(\mathbf{1})_2]^{2+}$ (534.5), $[Cu(\mathbf{1})\text{+CH}_3\text{CN}]^+$ (574.5), $[Cu_2(\mathbf{1})_3]^{2+}$ (769.3), $[Cu(\mathbf{1})_2]^+$ (1004.0), and $[Cu_2(\mathbf{1})_2PF_6]^+$ (1211.7). The mass spectra of **1** with Ag(I) salts exhibited a similar $M_nL_m$ fragment peak distribution (*m/z*): $[Ag(\mathbf{1})\text{+MeCN}]^+$ (618.4), $[Ag_2(\mathbf{1})_3]^{2+}$ (813.3), and $[Ag(\mathbf{1})_2]^+$ (1049.7) respectively, across all samples, as well as counterion specific peaks for $[Ag_2(\mathbf{1})_2]^{2+}$ (578.2), $[Ag(\mathbf{1})_2PF_6]^+$ (1301.4), $[Ag(\mathbf{1})_2SbF_6]^+$ (1391.3) for X = $[PF_6]^-$, $[SbF_6]^-$ and $[Ag_3(\mathbf{1})_4]^{3+}$ (733.9) for X = $[CB_{11}HCl_{11}]^-$. The compositions were further confirmed by comparison of experimental and theoretical isotopic distribution patterns. Notably, no $M_4L_4X_n$ ion was apparent for any sample.

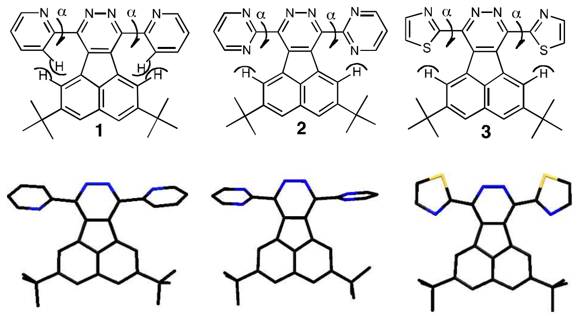


**Fig. 2** Structures of diazafluoranthene derivatives employed in the complexation reactions

**Scheme 1.** Synthesis of Ag(I) and Cu(I) complexes of **1-3**

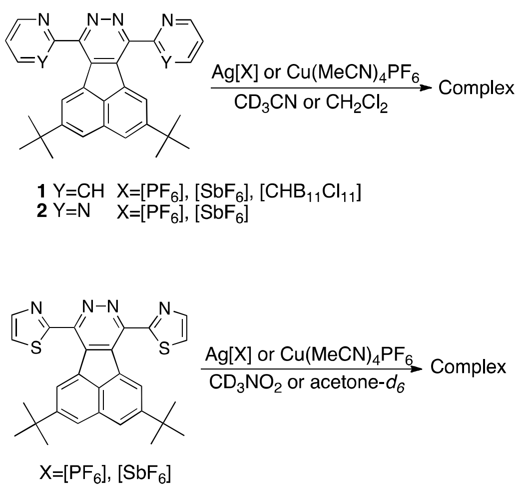


The ESI MS data of the dark red solution of **2** with Cu(I) in acetone showed ion signals (*m/z*) for the species $[Cu_2(\mathbf{2})_2]^{2+}$ (536.5), $[Cu_2(\mathbf{2})_3]^{2+}$ (772.5), and $[Cu(\mathbf{2})_2]^{+}$ (1008.0). Combinations of **2** with Ag(I) in acetonitrile exhibited peaks for $[Ag_2(\mathbf{2})_2]^{2+}$ (620.5), $[Ag_2(\mathbf{2})_3]^{2+}$ (816.5), and $[Ag(\mathbf{2})_2]^{+}$ (1054.0) plus counterion specific peaks for $[Ag_2(\mathbf{3})_2PF_6]^{+}$ (1305.6) and $[Ag_2(\mathbf{2})_2SbF_6]^{+}$ (1397.8). As with the complexes of **1**, there was no evidence of tetranuclear species in any solution.

A similar picture evolved from the mass spectra of **3** with Cu(I) and Ag(I) salts. The species $[Cu(\mathbf{3})_2]^{+}$, $[Cu(\mathbf{3})+CH_3CN+acetone+H]^{+}$ and $[Cu(\mathbf{3})+CH_3CN]^{+}$ at *m/z* 1027.9, 645.3 and 586.4, respectively, were observed for Cu(I) salts and $[Ag(\mathbf{3})_3]^{+}$ (1556.8), $[Ag(\mathbf{3})+MeCN+ H]^{+}$ (632.3) and $[Ag(\mathbf{3})_2]^{+}$ (1073.5) for Ag(I) salts, with counterion specific signals for $[Ag_2(\mathbf{3})_2PF_6]^{+}$ (1325.2) and $[Ag_2(\mathbf{3})_2SbF_6]^{+}$ (1417.7).

No tetranuclear complex was seen under MS conditions, but crystallography reveals a different story.

**X-ray crystallographic studies.** Representative crytsals were obtained for the free ligands **1-3**, as well as from every class in the array* (ligand **1-3** × $[Cu(CH_3CN)_4]PF_6$/AgX, X = $PF_6$, $SbF_6$, $CHB_{11}Cl_{11}$) to provide a comparison set of twelve structures.

The crystal structures of the ligands **1** and **2** (Fig. 2) consist of planar diazafluoranthene cores to which the pyridyl and pyrimidyl rings are inclined. The two pyridyl rings in **1** adopt a NC–CN *transoid* geometry; one is *syn clinal* to the central pyridazine ring (N–C–C–N torsion angle, α = 58.07(18)°), while the other is *anti clinal* (α = 132.15(18)°). In **2**, α = -68.7(2)° and 85.8(2)° for the pyrimidyl N-atoms closest to being *syn-periplanar* to the pyridazine ring. There are two symmetry-independent molecules in the structure of **3**; both are planar with an *anti-periplanar* disposition of the N-atoms and there is no obvious evidence to suggest that this is merely a consequence of averaging of superimposed twisted molecules.

A tetranuclear [2×2] grid-like architecture was observed cystallographically only from the reaction of $[Cu(CH_3CN)_4]PF_6$ with ligand **2**. A single crystal was obtained from a solution in acetone/methanol and the crystal structure determination indicated the formation of the $[Cu_4(\mathbf{2})_4][PF_6]_4\oplus2.17H_2O$ complex (**I**) (Fig. 3 and 4).

The asymmetric unit contains two tetranuclear cations, eight $PF_6^-$ anions, four sites fully occupied by water molecules and one site occupied by approximately one-third of a water molecule. Due to the absence of crystallographic symmetry within the cations, there are four different Cu···Cu separations in each cation in the range 3.2777(13)-3.4637(13) Å. Each Cu(I) ion is coordinated by two different ligands of **2** in a distorted tetrahedral geometry, and the Cu–N (pyridazine) and Cu–N (pyrimidine) distance are in the ranges 1.969(5)-2.022(5) Å and 1.987(5)-2.060(5) Å, respectively.

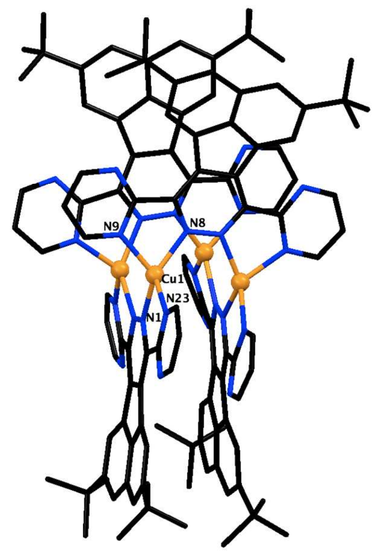


**Fig. 3** [2x2] grid-type structure of one of the two symmetry-independent cationic $[Cu_4(\mathbf{2})_4]^{4+}$ units present in $[Cu_4(\mathbf{2})_4][PF_6]_4\oplus2.17H_2O$ (**I**) (hydrogen atoms and counter ions have been omitted for clarity). Selected bond distances (Å) and angles (°): Cu1—N1 1.980(5), Cu1—N8 1.995(5), Cu1—N9 2.021(5), Cu1—N23 2.024(5), N1—Cu1—N23 79.9(2), N8—Cu1—N23 121.1(2), N9—Cu1—N8 80.5(2), N9—Cu1—N1 127.4(2), N8—Cu1—N1 136.5(2), N9—Cu1—N23 115.7(2)

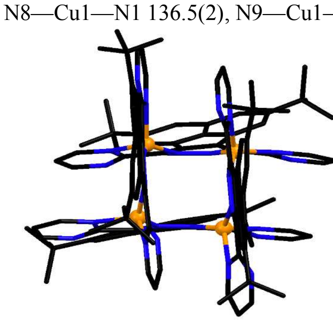

*Exception: the reaction of **3** with $AgSbF_6$

**Fig. 4** Top view of the grid-type structure of $[Cu_4(\mathbf{2})_4][PF_6]_4 \oplus 2.17H_2O$ (**I**) (hydrogen atoms and counter ions have been omitted for clarity).

The reaction of ligand **1** with one equivalent of $[Cu(CH_3CN)_4]PF_6$ in acetone resulted in the formation of a dark red solution. Crystals of the tetranuclear $[Cu_4(\mathbf{1})_4][PF_6]_4 \cdot 8C_3H_6O$ complex (**II**) with a saddle architecture were obtained from a solution in acetone/pentane. The solid-state structure of the cationic unit $[Cu_4(\mathbf{1})_4]^{4+}$ is presented in Fig. 5. The asymmetric unit contains one tetranuclear Cu-complex cation, four $PF_6^-$ anions and an estimated eight acetone molecules, some of which are highly disordered. In the cation, each Cu atom is coordinated by three different ligands in a distorted tetrahedral geometry, and the Cu-N (pyridazine) and Cu-N (pyridine) distances are in the ranges 1.948(4)-2.088(4) Å and 2.019(4)-2.125(4) Å respectively.

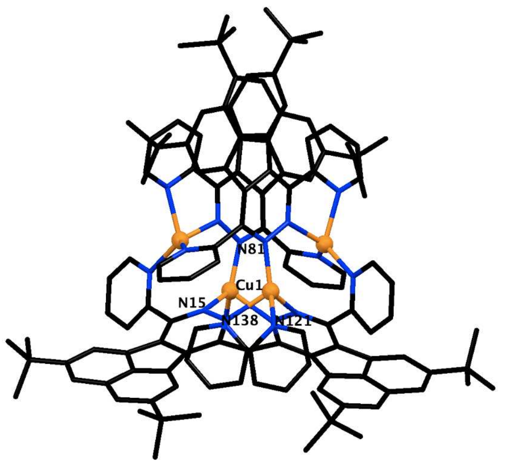


**Fig. 5** The solid state structure of the $[Cu_4(\mathbf{1})_4]^{4+}$ cation present in $[Cu_4(\mathbf{1})_4][PF_6]_4 \cdot 8C_3H_6O$ (**II**) (hydrogen atoms, counterions and solvent molecules have been omitted for clarity). Selected bond distances (Å) and angles (°): Cu1—N15 2.075(4), Cu1—N81 1.953(4), Cu1—N121 2.075(4), Cu1—N138 2.046(4), N15—Cu1—N138 107.5(2), N138—Cu1—N121 79.5(2), N121—Cu1—N15 94.3(2), N121—Cu1—N81 115.0(2), N81—Cu1—N138 124.1(2), N81—Cu1—N15 123.4(2)

In the grid structure $[Cu_4(\mathbf{2})_4]^{4+}$ each Cu atom is coodinated in a bidentate fashion by the pyridazine and pyrimidine N atoms of each of two ligands and each ligand bridges two different pairs of Cu atoms (bis-bidentate-bridging). In contrast, each ligand in the saddle-shaped $[Cu_4(\mathbf{1})_4]^{4+}$ cation is coordinated in a bidentate fashion to one Cu atom and is monodentate to each of two other Cu atoms, while two Cu atoms are coordinated by one pyridazine N atom from each of three ligands, plus one pyridine N atom from one of these ligands, while the other two Cu atoms are coordinated in the reverse way.

The combination of ligand **3** and $[Cu(CH_3CN)_4]PF_6$ did not present a product which gave cleanly interpretable $^1$H-NMR spectra; however, the solid state structure confirmed the formation of the tetranuclear species $[Cu_4(\mathbf{3})_4][PF_6]_4 \cdot 2CHCl_3 \cdot 2C_3H_6O$ (**III**) with the same saddle architecture as in $[Cu_4(\mathbf{1})_4][PF_6]_4 \cdot 8C_3H_6O$ (Fig. 6). Red crystals were obtained from a solution in acetone/chloroform/diethyl ether. The asymmetric unit contains one half of a $C_2$-symmetric disordered tetranuclear Cu-complex cation, two $PF_6^-$ anions and one disordered molecule of each of chloroform and acetone. As in $[Cu_4(\mathbf{1})_4][PF_6]_4 \cdot 8C_3H_6O$, each Cu atom is coordinated by three different ligands in a distorted tetrahedral geometry, and the Cu-N (pyridazine) and Cu-N (thiazole) distances are in the ranges 1.921(7)-2.197(6) Å and 1.954(7)-2.126(7) Å, respectively.

Reactions of the 7,10-disubstituted diazafluoranthene derivatives with silver salts Ag[X] (X = $[PF_6]^-$, $[SbF_6]^-$ and $[CB_{11}HCl_{11}]^-$) afforded complexes with three different motifs. Mixing 2,5-di-*tert*-butyl-7,10-di(pyridin-2-yl)-8,9-diazafluoranthene (**1**) and $[Ag][CHB_{11}Cl_{11}]$ resulted in the formation of the dinuclear $[Ag_2(\mathbf{1})_2][CHB_{11}Cl_{11}]_2 \oplus 4C_6H_4Cl_2 \oplus CH_2Cl_2$ complex (**IV**), which crystallized from dichloromethane/dichlorobenzene/hexane (Fig. 7).

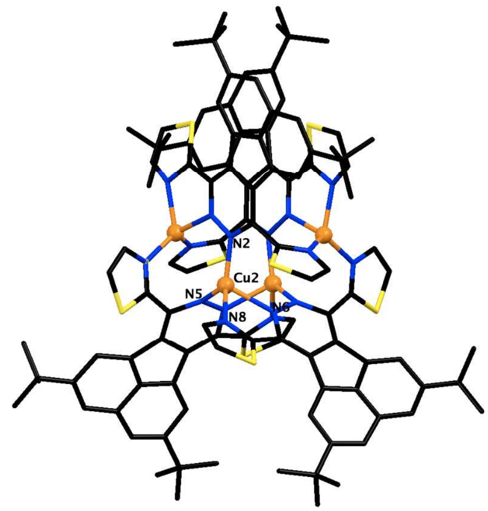


**Fig. 6** The solid state structure of the $[Cu_4(\mathbf{3})_4]^{4+}$ cation present in $[Cu_4(\mathbf{3})_4][PF_6]_4 \cdot 2CHCl_3 \cdot 2C_3H_6O$ (**III**) (hydrogen atoms, minor disorder conformation, counter-ion and solvent molecules have been omitted for clarity

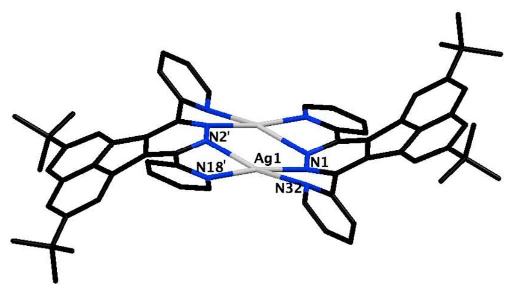


**Fig. 7** The solid state structure of the $[Ag_2(\mathbf{1})_2]^{2+}$ cation present in $[Ag_2(\mathbf{1})_2][CHB_{11}Cl_{11}]_2 \oplus 4C_6H_4Cl_2 \oplus CH_2Cl_2$ (**IV**). (The $[CHB_{11}Cl_{11}]^-$ anion, hydrogen atoms and and solvent molecules have been omitted for clarity). Selected bond distances (Å) and angles (°): Ag1—N1 2.240(2), Ag1—N2' 2.478(2), Ag1—N18' 2.254(2), Ag1—N32 2.602(2), N1—Ag1—N2' 115.10(5), N1—Ag1—N32 72.55(5), N2'—Ag1—N18' 70.95(5), N18'—Ag1—N32 103.24(5), N1—Ag1—N18 171.62(6), N2'—Ag1—N32 163.45(5); primed atoms are at the symmetry-related position 1-*x*, 1-*y*, -*z*

The use of silver salts with the smaller $[PF_6]^-$ and $[SbF_6]^-$ anions and the acetonitrile/benzene/hexane system for crystallization led to the tetranuclear $[Ag_4(\mathbf{1})_4][PF_6]_4 \cdot 3C_6H_6 \cdot 4CH_3CN$ (**V**) and $[Ag_4(\mathbf{1})_4][SbF_6]_4 \cdot 4C_5H_{12}$ (**VI**) complexes that have essentially isostructural cations, but do not exhibit a grid-type architecture (Fig. 8). In the former, the cation has crystallographic inversion symmetry, while that in the latter has crystallographic $C_{2h}$ symmetry. In the cation, two ligands coordinate two Ag-atoms each in a bidentate mode involving one pyridazine and one pyridine N atom and simultaneously bridge these Ag atoms through the pyridazine N atoms, while each of the other two ligands coordinate in a bridging-monodentate fashion to all four Ag atoms. As a result, each Ag atom is coordinated by three different ligands and is found to adopt a somewhat flattened tetrahedral geometry. The four silver atoms are at the corners of a rectangle, with sides of

5.0623(4) Å and 3.8761(4) Å ($[PF_6]^-$ salt), and 4.9727(3) Å and 3.8839(3) Å ($[SbF_6]^-$ salt).

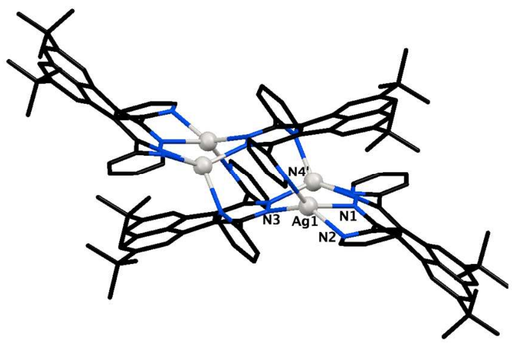


**Fig. 8** The structure of the tetranuclear $[Ag_4(\mathbf{1})_4]^{4+}$ cation present in $[Ag_4(\mathbf{1})_4][SbF_6]_4{\cdot}4C_5H_{12}$ (**VI**) (hydrogen atoms, counter ions and solvent molecules have been omitted for clarity). Selected bond distances (Å) and angles (°): Ag1—N1 2.363(2), Ag1—N2 2.398(2), Ag1—N3 2.343(2), Ag1—N4' 2.413(2), N1—Ag1—N2 72.17(8), N2—Ag1—N3 141.07(9), N3—Ag1—N4' 102.67(8), N4'—Ag1—N2 99.41(8), N1—Ag1—N3 109.72(8), N4'—Ag1—N1 136.97(8); primed atoms are at the symmetry-related position 1-*x*, *y*, -*z*

2,5-di-*tert*-butyl-7,10-di-(pyrimidin-2-yl)-8,9-diaza-fluoranthene (**2**) affords crystals of dinuclear complexes with $AgPF_6$ and $AgSbF_6$. The cations in $[Ag_2(\mathbf{2})_2][PF_6]_2{\cdot}0.5CH_2Cl_2{\cdot}0.5C_6H_5Cl{\cdot}0.5C_6H_{14}$ (**VII**) and $[Ag_2(\mathbf{2})_2][SbF_6]_2{\cdot}C_3H_6O{\cdot}0.5C_6H_6{\cdot}0.5C_6H_{14}$ (**VIII**) are almost isostructural, and in both cases, consist of two Ag(I) ions (Ag···Ag separations are 3.5431(5) and 3.5292(5) Å, respectively), each coordinated by four nitrogen atoms from two ligands in a slightly distorted square-planar arrangement (Fig. 9), in a similar way to that observed for $[Ag_2(\mathbf{1})_2][CHB_{11}Cl_{11}]_2{\oplus}4C_6H_4Cl_2\ {\oplus}CH_2Cl_2$. The cation in the $[PF_6]^-$ salt sits across a crystallographic mirror plane perpendicular to the Ag···Ag axis, while that in the $[SbF_6]^-$ salt lies in a general position. The structures of the $[Ag_2(\mathbf{2})_2]^{2+}$ cations in these salts look similar to that observed for $[Ag_2(\mathbf{1})_2][CHB_{11}Cl_{11}]_2{\oplus}4C_6H_4Cl_2{\oplus}CH_2Cl_2$, although the entire dinuclear complex of $[Ag_2(\mathbf{2})_2]^{2+}$ is flatter than that of $[Ag_2(\mathbf{1})_2]^{2+}$, as a result of the absence of steric H···H repulsion across the bay region[15] in the ligand.

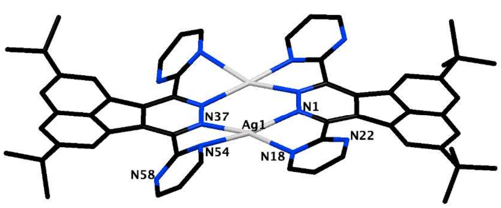


**Fig. 9** The structure of the $[Ag_2(\mathbf{2})_2]^{2+}$ cation present in $[Ag_2(\mathbf{2})_2][PF_6]_2{\cdot}0.5CH_2Cl_2{\cdot}0.5C_6H_5Cl{\cdot}0.5C_6H_{14}$ (**VII**) (hydrogen atoms and counter ions have been omitted for clarity). Selected bond distances (Å) and angles (°): Ag1—N1 2.360(3), Ag1—N18 2.366(3), Ag1—N37 2.305(3), Ag1—N54 2.561(3), N1—Ag1—N18 69.4(1), N18—Ag1—N54 101.7(1), N54—Ag1—N37 69.2(1), N37—Ag1—N1 121.9(1), N54—Ag1—N1 160.3(1), N18—Ag1—N37 167.7(1)

A single crystal of $[Ag_2(\mathbf{3})_2]_n[PF_6]_{2n}{\cdot}n(C_3H_6O)$ (**IX**) was obtained from acetone/nitromethane/hexane. The cation in this structure is a one-dimensional polymeric ribbon (Fig. 10). The asymmetric unit contains two $Ag^+$ ions, two ligands (**3**), two $[PF_6]^-$ anions and one acetone molecule. Although in such a polymeric cation the chemical repeat unit can be considered to be $[Ag(\mathbf{3})]^+$ , it is convenient to describe the structure in terms of the crystallographically unique segment of the polymer, *viz.* $[Ag_2(\mathbf{3})_2]^{2+}$. Firstly, the two unique silver atoms are coordinated by all four N-atoms from one ligand in a bis-bidentate-bridging fashion, as seen in several of the structures described above. A second ligand also bridges the same two Ag atoms through its two pyridazine N atoms (although the Ag1–N8 bond is quite long at 2.721(7) Å), but now the thiazole rings are oriented such that the thiazole N atoms do not coordinate with these two Ag atoms, but with two other symmetry-related Ag atoms. These last connections mean that each Ag atom is coordinated by three ligands and nominally by four N atoms. However, the twisting of the thiazole rings of the second ligand described above brings the two S-atoms close to the two Ag atoms of the asymmetric unit and these can be considered weak Ag···S interactions that might have some influence on the coordination geometry (Ag1···S2 = 3.162(3) and Ag2···S1 = 3.292(3) Å; shorter than the sum of the van der Waals radii of these atoms of 3.52 Å). The Ag–N distances in the polymeric cation span a wide range: 2.208(8)-2.720(7) Å. The coordination geometry at each indpendent Ag atom is so contorted (Fig. 10), that it is unrealistic to attempt to assign a classical geometry descriptor to these.

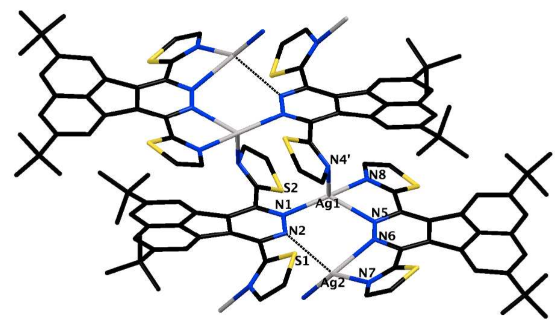


**Fig. 10** Crystal structure of polymeric cation $[Ag_2(\mathbf{3})_2]^{2+}$ present in $([Ag_2(\mathbf{3})_2]^{2+})_n{\cdot}2nPF_6{\cdot}nC_3H_6O$ (**IX**) (hydrogen atoms, counter ions and solvent molecules have been omitted for clarity). Selected bond distances (Å) and angles (°): Ag1—N1 2.247(7), Ag1—N4' 2.506(8), Ag1—N5 2.348(7), Ag1—N8 2.258(7), Ag1—S2 3.161(3) N1—Ag1—N4 87.1(3), N4—Ag1—N8 112.2(3), N4—Ag1—N5 94.0(3), N1—Ag1—N8 158.7(3), N4'—Ag1—N5 94.0(3), N1—Ag1—N5 120.6 (2), Ag2—N7 2.285(7), Ag2—N6 2.371(7), Ag2—N2 2.720(7), Ag2—S1 3.292(3), N7—Ag2—N6 70.5(3), N7—Ag2—N2 133.2(3), N6—Ag2—N2 99.5(2)

The NMR and MS data from the reaction of **3** with $AgSbF_6$ support the formation of the same polymeric structure as with $AgPF_6$. Attempts to isolate crystals of the $[SbF_6]^-$ salt were unsuccessful.

**Conformational analysis.** The N/S donor atoms in ligands **1-3** act in mono- and bidentate coordination modes with $[Cu(CH_3CN)_4]PF_6$ and three different silver(I) salts, resulting in the formation of the nine reported structures **I-IX** (three Cu(I) and six Ag(I) salts), which display distorted tetrahedral coordination at each Cu(I) ion and distorted tetrahedral or square planar coordination geometry at the Ag(I) ions.

The structural diversity of the Cu(I) and Ag(I) metal complexes is associated with the flexible coordination chemistry of these closed shell $d^{10}$ metal ions, considered to provide linear, tetrahedral or square planar coordination geometries. A measure of the degree of distortion of a four-coordinate metal system from the ideal extremes of tetrahedral and square planar is Houser's $\tau_4$ parameter,[16] which varies from 0.0 for perfect square planar to 1.0 for ideal tetrahedral geometry. In addition, ligand N–C–C–N torsion angles, α, involving the pyridazine and terminal aryl rings in each compound and complex were evaluated. These structural data, as well as the metal identity, the constitutional nature of the ligands, the molecular ratio of metals to ligand overall, the ligand field around the metal, the chelation mode of the polydentate ligand, the nature of the anion and the symmetry of the complexes are summarized in Table 1.

**Table 1. Taxonomy of Cu(I) and Ag(I) complexes with diarylpyridazines**

| Complex | Metal | Ligand Type | M:L | $\tau_4$ (°) | Ligand Field | Chelation # | Ligand Config | Metal Array Geometry | Symmetry Local (Crystallographic) | Anion |
|---|---|---|---|---|---|---|---|---|---|---|
| **1** | --- | N/CH | | | | | sp / ac | | $C_2$ $(C_1)$ | |
| **2** | --- | N/N | | | | | sp / ac | | $C_s$ $(C_1)$ | |
| **3** | --- | N/S | | | | | ap / ap | | $C_{2v}$ $(C_{2v}, Cs)$ | |
| **I** | Cu | **2** | 4:4 | 0.66-0.71 | td | 4[2+2] | sp / sp | Tetranuclear planar | $D_2$ $(C_1)$ | $PF_6^-$ |
| **II** | Cu | **1** | 4:4 | 0.80-0.84 | td | 4[2+2] [2+1+1] | sp / sc sp / cc | Tetranuclear saddle | $C_2$ $(C_1)$ | $PF_6^-$ |
| **III** | Cu | **3** | 4:4 | 0.83 | td | 4[2+2] [2+1+1] | sp / sc sp / cc | Tetranuclear saddle | $C_2$ $(C_2)$ | $PF_6^-$ |
| **IV** | Ag | **1** | 2:2 | 0.18 | sq pl | 4[2+2] | sp / sc | Dinuclear planar | ~ $C_{2h}$ $(C_i)$ | $CHB_{11}Cl_{11}^-$ |
| **V** | Ag | **1** | 4:4 | 0.57-0.58 | 'flat' td | 4[2+1+1] [1+1+1+1] | sp / ac | Tetranuclear planar | $C_{2h}$ $(C_i)$ | $PF_6^-$ |
| **VI** | Ag | **1** | 4:4 | 0.58 | 'flat' td | 4[2+1+1] [1+1+1+1] | sp / ac | Tetranuclear planar | $C_{2h}$ $(C_{2h})$ | $SbF_6^-$ |
| **VII** | Ag | **2** | 2:2 | 0.23-0.26 | sq pl | 4[2+2] | sp / sp | Dinuclear planar | ~ $C_{2h}$ $(C_1)$ | $PF_6^-$ |
| **VIII** | Ag | **2** | 2:2 | 0.24 | sq pl | 4[2+2] | sp / sp | Dinuclear planar | ~ $C_{2h}$ $(C_s)$ | $SbF_6^-$ |
| **IX** | Ag | **3** | 1:1 | | | 4[2+2] [1+1+1+1] | sp / sp a' / a' | Polymer | $C_i$ $(C_i)$ | $PF_6^-$ |

Ligand Conformation: sp = syn-periplanar with angle under 30°, sc = syn clinal with angle between 30 and 90°, cc = clinal for angles very close to 90°, ac = anti clinal with angle between 90 and 150°, ap = anti-periplanar with angle over 150°, a' = 135°. Chelation # refers to the number of heteroatoms around the metal [contribution per ligand]. Metal Array Geometry refers to the collection of metal positions in the complex and not the ligand field.

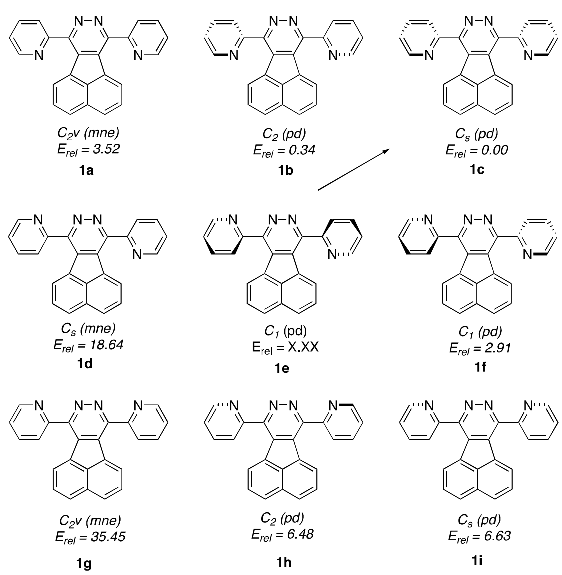


**Fig. 11** Relative energies of the possible conformations of **1**

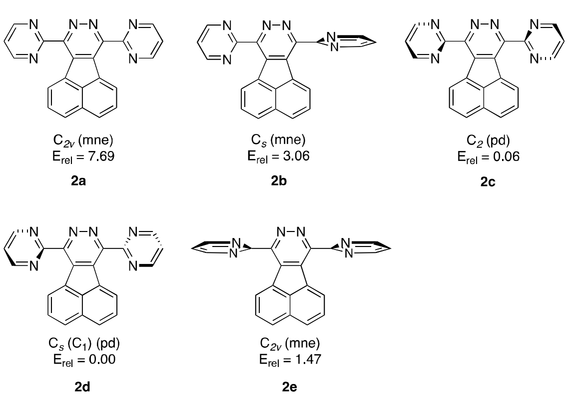


**Fig. 12** Relative energies of the possible conformations of **2**

Introduction of a second nitrogen atom into the aryl substituents decreases the relative energy of the N-*syn clinal* conformation. Computational analysis suggests five structural conformations for ligand **2** (Fig. 12). Structural diversity is represented by the totally planar structure **2a**, which has the highest relative energy of 7.69 kcal/mol, structure **2b** with a *sc/ap* conformation of one aryl group and a *cc* conformation of the second, stucture **2e** with an orthogonal arrangement of both pyrimidine rings (presented in the crystal structure of **2**), and the energetically favorable coformations **2c** and **2d**. Structures **2d** and **2a** were components in the construction of the molecular grid **I** and dinuclear structures **VII**, **VIII**.

Computational analysis of ligand **3** resulted in only three structural possibilities for the thiazole system **3a-c** (Fig. 13). All structures are planar in this case, with the enegy minima having an *anti-periplanar* conformation, **3a**, as observed in the crystal structure of **3**. All other possible conformations of **3** are predicted to interconvert to one of the three planar structures **3a-c**.

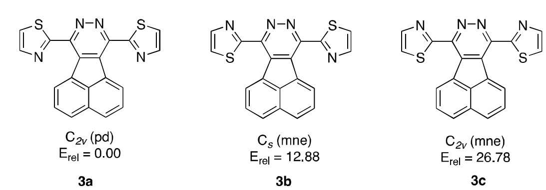


**Fig. 13** Relative energies of the possible conformations of **3**

Replacement of the sulfur atoms in **3** by oxygen, resulted in nine conformational isomers **4a-i** (Fig. 14), where **4e** interconverts into the energetically favorable conformation **4b** (0.11 kcal/mol). Here, **4b** and **4h** can be used as reference structures for the polymeric complex **IX**, whereas the ligand conformation in **III** can be represented by the reference structures **4h** and **2b**. Rotation of the oxazole groups from the *anti-periplanar* into the *syn clinal* conformations is seen to increase the energy of the system, as shown in Fig. 14.

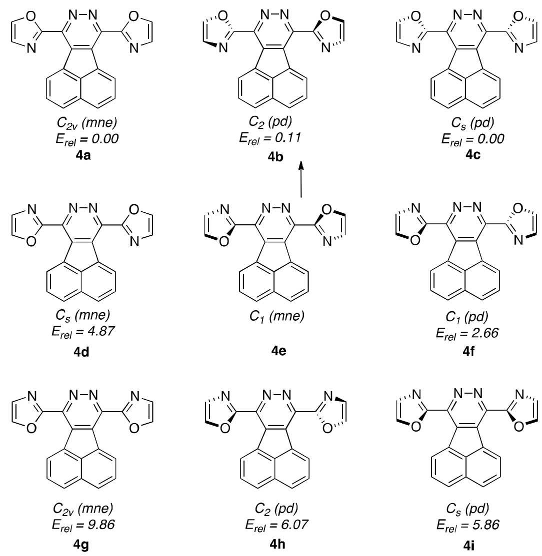


**Fig. 14** Relative energies of the possible conformations of **4**

## Conclusion

Investigation of the complexation reactions of 7,10-disubstituted diazafluoranthene derivatives with three different silver salts and $[Cu(CH_3CN)_4]PF_6$ led to an array of structures inconsistent with any simple rules, such as maximum ligand occupancy, or prefered coordination geometry.[17] ESI MS spectra of these reaction solutions provided no evidence for tetranuclear species (except for complex IV). Although mixtures of $M_xL_y$ could not be excluded in solution, clearly no unique "programmed" complex is formed. The crystal structures of 2,5-di-*tert*-butyl-7,10-di(pyridin-2-yl)-8,9-diazafluoranthene (**1**) with Ag(I) and Cu(I) salts displayed three structural motifs. The use of relatively small anions, namely $[PF_6]^-$ and $[SbF_6]^-$, led to the formation of tetranuclear complex cations as their $[Ag_4(\mathbf{1})_4][X]_4$ and $[Cu_4(\mathbf{1})_4][PF_6]_4$ salts whose structures are not of the grid-type, but have a "proppeller" and saddle-type shape. The larger $[CHB_{11}Cl_{11}]^-$ anion crystallized with a wave-like dinuclear cation in $[Ag_2(\mathbf{2})_2][CHB_{11}Cl_{11}]_2$. 2,5-Di-*tert*-butyl-7,10-di-(pyrimidin-2-yl)-8,9-diazafluoranthene (**2**) and 2,5-di-*tert*-butyl-7,10-di(thiazol-2-yl)-8,9-diazafluo-ranthene (**3**), which are less hindered in terms of *H*–heterocycle repulsion, afforded crystals of dinuclear and polymeric complexes with $AgPF_6$ and $AgSbF_6$, and a saddle-type tetranuclear complex $[Cu_4(\mathbf{3})_4][PF_6]_4$. A grid structure was obtained only for crystals of **I** obtained from 2,5-di-*tert*-butyl-7,10-di-(pyrimidin-2-yl)-8,9-diazafluo-ranthene (**2**) and $[Cu(CH_3CN)_4]PF_6$.

Quantum mechanical calculations of the relative energies for the possible structural conformations of **1**, **2**, **3** and oxazole disubstituted diazafluoranthenes **4** have shown the *anti-periplanar* conformation of the ligands to be energetically preferable; in the complexes *syn-periplanar* conformations predominate.

It has been previously noted that "programmed ligand-metal architectures" are more often artifact than algorithmic based.[17b,d-f] The present study focuses on a class of cognate components, which might be presumed to all give a similar "prgrammed" outcome, but for which 'exception' seems to be the rule.

## Experimental

**General information:** All solvents were used as purchased (p. a. grade) without further purification. Commercially available chemicals were used as purchased without further purification. Melting points were determined using a Büchi B-540 melting point apparatus and are uncorrected. Infrared spectra were recorded on a Perkin-Elmer Spectrum One FT-IR spectrometer. Compounds were measured as KBr pellets. Absorption bands are given in wave-numbers ($cm^{-1}$), and the intensities are characterized as follows: *s* = strong (0-33% transmission), *m* = medium (34-66% transmission), *w* = weak (67-100% transmission). UV-Vis absorption spectra (250-650 nm) were collected on an Agilent 8453 UV-Vis spectrophotometer. $^1$H- and $^{13}$C-NMR spectra were recorded on Bruker Avance 400 (400 MHz), Bruker Avance 500 (500 MHz), Bruker DRX-500 (500 MHz) and Bruker DRX-600 (600 MHz) spectrometers, with the solvent as the internal standard. Data are reported as follows: chemical shift in ppm, multiplicity (*s* = singlet, *d* = doublet, *m* = multiplet, *dd* = doublet of doublets, *dt* = doublet of triplet, *etc.*), coupling constant $^nJ$ in Hz, integration and interpretation. Mass spectra (MS) were obtained from a Finnigan MAT95 instrument. Analytical thin layer chromatography (TLC) was performed with Macherey-Nagel POLYGRAM SIL N-HR/$UV_{254}$ and POLYGRAM ALOX N/$UV_{254}$, visualization by an ultraviolet (UV) lamp ($\lambda$ = 254 nm and $\lambda$ = 366 nm). Column chromatography was carried out on silica gel (Merck silica gel 60 (particle size 0.040 - 0.063 mm). Complexation reactions were carried out using stoichiometric amounts of silver(I) salts Ag[X] (X = $[PF_6]^-$, $[SbF_6]^-$, $[CHB_{11}Cl_{11}]^-$), $[Cu(CH_3CN)_4]PF_6$ and diazafluoranthene ligands. $^1$H-NMR of these reactions indicated full conversion to the silver and copper complexes of **1**, **2** and **3**.

**2,5-Di-*tert*-butyl-7,10-di(pyridin-2-yl)-8,9-diazafluo-ranthene (1)**. A mixture of 3,6-di(pyridin-2-yl)-1,2,4,5-tetrazine (0.36 g, 1.52 mmol) and 4,7-di-*tert*-butylacenaphthylene (0.2 g, 0.76 mmol) in $CH_2Cl_2$ (20 mL) was stirred at reflux overnight. The solvent was evaporated, the residue was purified by column chromatography (silica gel, hexane/ethyl acetate 10:1→5:1→1:1) to yield a yellow solid (0.34 g, 95%). IR (KBr): 3064*m*, 2961*s*, 2904*s*, 2886*s*, 1624*w*, 1587*s*, 1566*s*, 1552*w*, 1538*m*, 1475*s*, 1443*s*, 1434*s*, 1393*m*, 1369*s*, 1325*s*, 1290*m*, 1244*m*, 1224*m*, 1210*m*, 1155*m*, 1116*m*, 1093*s*, 1084*s*, 1041*m*, 1022*w*, 925*m*, 894*m*, 822*w*, 800*m*, 787*s*, 749*s*, 684*m*, 664*m*, 638*m*, 614*m*, 591*w*, 569*w*, 406*w*; $^1$H-NMR (500 MHz, $CD_3CN$) δ 8.96 (ddd, 1H, $^3J$ = 4.8, $^4J$ = 2.0, $^5J$ = 1.2 Hz), 8.59 (d, 1H, $^4J$ = 1.6 Hz), 8.32 (dt, 1H, $^3J$ = 8.0, $^4J$ = 1.2), 8.13 (d, 1H, $^4J$ = 1.2 Hz), 8.10 (td, 1H, $^3J$ = 7.6, $^4J$ = 1.6 Hz), 7.64 (ddd, 1H, $^3J$ = 6.0, $^3J$ = 4.8, $^5J$ = 1.2 Hz), 1.43 (s, 9H); $^{13}$C-NMR (400 MHz, $CD_3CN$), δ 157.2, 156.0, 152.3, 149.5, 138.2, 136.1, 132.3, 130.1, 130.0, 128.2, 126.9, 125.5, 125.4, 36.5, 31.8; MS (ESI) m/z (%): 470.2 ($M^+$, 100), 455.2 ($M^+$-Me, 69), 439.2 (22), 414.2 (47%); HRMS (ESI) calcd. for $C_{32}H_{30}N_4$: 470.2470; found: 470.2459; UV–Vis ($CH_2Cl_2$), $\lambda_{max}$ nm (log ε): 247 (4.7), 276 (4.5), 312 (4.2), 329 (4.1), 376 (4.1); mp. 290 °C.

**2,5-Di-*tert*-butyl-7,10-di(pyrimidin-2-yl)-8,9-diazafluo-ranthene (2).** A mixture of 3,6-di(pyrimidin-2-yl)-1,2,4,5-tetrazine (0.54 g, 2.3 mmol) and 4,7-di-*tert*-butylacenaphthylene (0.3 g, 1.13 mmol) in DMSO (10 mL) was stirred at 100 °C overnight. The mixture was diluted with water (50 mL), the precipitate formed was filtered off, washed with methanol and dried to yield a yellow solid (0.45 g, 85%). IR (KBr): 2962*s*, 2869*m*, 1627*w*, 1599*w*, 1560*s*, 1445*s*, 1433*m*, 1424*m*, 1395*w*, 1371*s*, 1327*m*, 1264*w*, 1251*w*, 1231*m*, 1213*m*, 1185*w*, 1146*m*, 1132*w*, 1100*m*, 1081*m*, 1008*w*, 990*w*, 934*w*, 892*m*, 814*m*, 807*m*, 755*w*, 698*w*, 679*m*, 642*m*, 621*m*, 590*w*, 566*w*; $^1$H-NMR (400 MHz, $CD_2Cl_2$) δ 9.18 (s, 1H), 9.17 (s, 1H), 8.25 (d, 1H, $^4J$ = 1.2 Hz), 8.10 (d, 1H, $^4J$ = 1.2), 7.63 (dd, 1H, $^3J$ = 4.8, $^3J$ = 4.8 Hz), 1.4 (s, 9H); $^{13}$C-NMR (400 MHz, $CD_2Cl_2$), δ 165.1, 158.3, 154.5, 152.2, 136.2, 131.4, 130.2, 129.9, 127.3, 127.0, 122.0, 36.1, 31.9; MS (ESI) m/z (%): 472.2 ($M^+$,100), 457.2 ($M^+$-Me, 98), 441.2 ($M^+$-2Me+H, 29), 416.2 ($M^+$-3Me+H, 30), 401.2 (6), 228.6 (19%) ; HRMS (ESI) calcd. for $C_{30}H_{28}N_6$: 472.2375; found: 472.2378; UV - Vis ($CH_2Cl_2$), $\lambda_{max}$ nm (log ε): 244 (4.7), 307 (4.2), 326 (4.0), 373 (4.1); mp. over 350 °C.

**2,5-Di-*tert*-butyl-7,10-di(thiazol-2yl)-8,9-diazafluoran-thene (3)**. A mixture of 3,6-di(thiazol-2-yl)-1,2,4,5-tetrazine (0.092 g, 0.37 mmol) and 4,7-di-*tert*-butyl-acenaphthylene (0.05 g, 0.19 mmol) in dichloromethane (3 mL) was stirred at reflux for four hours. The solvent was evaporated and the residue was purified by column chromatography (silica gel, hexane/ethyl acetate 10:1) to yield a yellow solid (0.056 g, 63%). IR (KBr): 3121*w*, 3073*w*, 2948*s*, 2857*s*, 1867*w*, 1725*m*, 1624*w*, 1557*w*, 1525*w*, 1498*m*, 1477*s*, 1463*s*, 1443*s*, 1423*s*, 1395*s*, 1368*s*, 1332*s*, 1323*m*, 1309*s*, 1289*m*, 1268*s*, 1227*s*, 1220*s*, 1208*m*, 1183*m*, 1088*m*, 1059*m*, 1033*s*, 1020*m*, 963*s*, 935*m*, 898*s*, 875*s*, 845*s*, 799*s*, 721*s*, 668*s*, 641*s*, 599*w*, 581*m*, 561*m*, 481*w*; $^1$H-NMR (500 MHz, $CDCl_3$) δ 10.21 (d, 1H, $^4$J = 1.5), 8.26 (d, 1H, $^3$J = 3.0) 8.16 (d, 1H, $^4$J = 1.0 Hz), 7.68 (d, 1H, $^3$J = 3.0 Hz) 1.59 (s, 9H); $^{13}$C-NMR (400 MHz, $CD_2Cl_2$), δ 168.2, 152.1, 150.1, 143.9, 134.4, 131.1, 131.0, 130.1, 129.2, 126.9, 123.0, 36.1, 32.0; MS (ESI) m/z (%): 482.1 ($M^+$, 60%), 467.1 ($M^+$-$CH_3$, 100), 451.1 (16), 427.1 (13%) ; HRMS (ESI) calcd. for $C_{28}H_{26}N_4S_2$: 482. 1599; found: 482.1592; UV - Vis ($CH_2Cl_2$), $\lambda_{max}$ nm (log ε): 235 (4.6), 311 (4.5), 327 (4.5), 386 (4.2); mp. 170 °C decomp.

**$[Cu_4(2)_4][PF_6]_4$ (I)**. A mixture of 2,5-di-*tert*-butyl-7,10-di-(pyrimidin-2-yl)-8,9-diazafluoranthene (**2**) (0.05 g, 0.106 mmol) and $[Cu(CH_3CN)_4]PF_6$ (0.04 g, 0.106 mmol) in acetone-$d_6$ (2 mL) was stirred at RT overnight. The mixture turned dark red right after the addition of the solvent. $^1$H-NMR (500 MHz, acetone-$d_6$) δ 9.70 (s, 1H), 9.10 (s, 2H), 8.50 (s, 1H), 7.76 (s, 1H), 1.48 (s, 9H); $^{13}$C-NMR (500 MHz, $CD_3CN$), δ 159.9, 158.5, 153.3, 150.4, 140.6, 134.4, 131.8, 131.6, 130.3, 129.7, 125.0, 36.6, 32.2; MS (ESI) m/z (%): 1008.0 ($[Cu(C_{30}H_{28}N_6)_2]^+$, 3), 772.5 ($[Cu_2(C_{30}H_{28}N_6)_3]^{2+}$, 20), 576.5 ($[Cu(C_{30}H_{28}N_6)+CH_3CN]^+$, 100), 473.4 ($[C_{30}H_{28}N_6+ H]^+$, 50), 457.3 ($[C_{30}H_{28}N_6$-Me$]^+$, 21%); UV - Vis ($CH_2Cl_2$), $\lambda_{max}$ nm (log ε): 243 (5.1), 336 (4.8), 472 (4.7).

**$[Cu_4(1)_4][PF_6]_4$ (II)**. A mixture of 2,5-di-*tert*-butyl-7,10-di(pyridin-2-yl)-8,9-diazafluoranthene (**1**) (0.02 g, 0.042 mmol) and $[Cu(CH_3CN)_4]PF_6$ (0.016 g, 0.042 mmol) in acetone-$d_6$ (3 mL) was stirred at RT overnight under an argon atmosphere. The mixture turned dark red right after the addition of the solvent. $^1$H-NMR (500 MHz, $CD_3CN$) δ 8.51 (s, 1H), 8.24 (s, 1H), 8.11 (s, 1H), 8.08 (s, 1H), 7.85 (s, 1H), 7.44 (s, 1H), 1.35 (s, 9H); $^{13}$C-NMR (500 MHz, $CD_3CN$) δ 153.5, 153.3, 153.0, 150.7, 138.4, 136.8, 130.7, 130.2, 128.8, 127.8, 127.4, 126.3, 126.3 36.4, 31.7; MS (ESI) m/z (%): 1476.4 ($[Cu(C_{32}H_{30}N_4)_3]^+$, 0.2), 1211.7 ($[Cu_2(C_{32}H_{30}N_4)_2PF_6]^+$, 0.3), 1004.0 ($[Cu(C_{32}H_{30}N_4)_2]^+$, 11), 769.3 ($[Cu_2(C_{32}H_{30}N_4)_3]^{2+}$, 6), 574.5 ($[Cu(C_{32}H_{30}N_4)$ +MeCN$]^+$, 87), 534.5 ($[Cu_2(C_{32}H_{30}N_4)_2]^{2+}$, 8), 471.4 ($[C_{32}H_{30}N_4$+H$]^+$, 100%); UV - Vis ($CH_2Cl_2$), $\lambda_{max}$ nm (log ε): 231 (5.2), 298 (4.9), 426 (4.8).

**$[Cu_4(3)_4][PF_6]_4$ (III)**. A mixture of 2,5-di-*tert*-butyl-7,10-di(thiazol-2yl)-8,9-diazafluoranthene (**3**) (0.01 g, 0.021 mmol) and $[Cu(CH_3CN)_4]PF_6$ (0.008 g, 0.021 mmol) in acetone-$d_6$ (1 mL) was stirred at RT overnight under an argon atmosphere. MS (ESI) m/z (%): 1027.9 ($[Cu(C_{28}H_{26}N_4S_2)_2]^+$, 31), 645.3 ($[Cu(C_{28}H_{26}N_4S_2)$+ $CH_3CN$+acetone+H$]^+$, 9), 586.4 ($[Cu(C_{28}H_{26}N_4S_2)$+ $CH_3CN]^+$, 100), 483.3 ($[C_{28}H_{26}N_4S_2$+H$]^+$, 12%); UV - Vis ($CH_2Cl_2$), $\lambda_{max}$ nm (log ε): 230 (5.2), 319 (4.9), 445 (4.8).

**$[Ag_2(1)_2][CHB_{11}Cl_{11}]_2$ (IV)**. A mixture of 2,5-di-*tert*-butyl-7,10-di(pyridin-2-yl)-8,9-diazafluoranthene (**1**) (0.019 g, 0.04 mmol) and $AgCHB_{11}Cl_{11}$ (0.025 g, 0,04 mmol) in $CD_3CN$ (1mL) was stirred at RT overnight. $^1$H-NMR (400 MHz, $CD_3CN$) δ 8.67 (s, 1H), 8.23 (s, 2H), 8.05 (s, 1H), 7.90 (s, 1H), 7.56 (s, 1H), 1.39 (s, 9H); $^{13}$C-NMR (400 MHz, $CD_3CN$), δ 154.2, 153.3, 152.9, 151.9, 138.3, 137.2, 130.31, 130.0, 129.7, 129.21, 127.1, 127.0, 126.8; MS (ESI) m/z (%): 1049.7 ($[Ag(C_{32}H_{30}N_4)_2]^+$, 2.5), 734.0 ($[Ag_3(C_{32}H_{30}N_4)_4]^{3+}$, 24), 620.3 ($[Ag(C_{32}H_{30}N_4)+CH_3CN]^+$, 17), 471.3 ($[(C_{32}H_{30}N_4)$+H$]^+$, 100%); UV–Vis ($CH_2Cl_2$), $\lambda_{max}$ nm (log ε): 231 (5.3), 281 (5.0), 328 (4.9), 409 (4.8).

**$[Ag_4(1)_4][PF_6]_4$ (V)**. A mixture of 2,5-di-*tert*-butyl-7,10-di(pyridin-2-yl)-8,9-diazafluoranthene (**1**) (0.03 g, 0.064 mmol) and $AgPF_6$ (0.016 g, 0.064 mmol) in $CD_3CN$ (3 mL) was stirred at RT overnight. $^1$H-NMR (400 MHz, $CD_3CN$) δ 8.30 (d, 1H, $^3$J = 4.4 Hz), 8.23 (d, 1H, $^4$J = 1.2 Hz), 7.84 (d, 1H, $^3$J = 7.6 Hz), 7.75 (s, 1H), 7.62 (dd, 1H, $^3$J = 7.6 Hz), 7.21 (dd, 1H, $^3$J = 5.2, $^3$J = 6.8 Hz), 1.33 (s, 9H); $^{13}$C-NMR (400 MHz, $CD_3CN$), δ 157.2, 156.0, 152.3, 150.0, 138.2, 136.1, 132.3, 130.1, 130.0, 128.2, 126.8, 125.5, 125.4, 36.2, 31.8; MS (ESI) m/z (%): 1049.7 ($[Ag(C_{32}H_{30}N_4)_2]^+$, 14), 813.4 ($[Ag_2(C_{32}H_{30}N_4)_3]^{2+}$, 21), 618.4 ($[Ag(C_{32}H_{30}N_4)$ + MeCN$]^+$, 100), 578.2 $[Ag_2(C_{32}H_{30}N_4)_2]^{2+}$ (18), 471.3 $[(C_{32}H_{30}N_4)$+H$]^+$ (46), 455.2 $[(C_{32}H_{30}N_4)$-Me+H$]^+$ (36%); UV - Vis ($CH_2Cl_2$), UV - Vis ($CH_3CN$), $\lambda_{max}$ nm (log ε): 245 (5.2), 276 (5.0), 312 (4.7), 327 (4.6), 374 (4.7).

**$[Ag_4(1)_4][SbF_6]_4$ (VI)**. A mixture of 2,5-di-*tert*-butyl-7,10-di(pyridin-2-yl)-8,9-diazafluoranthene (**1**) (0.03 g, 0.064 mmol) and $AgSbF_6$ (0.022 g, 0.064 mmol) in $CD_3CN$ (3 mL) was stirred at RT overnight. $^1$H-NMR (400 MHz, $CD_3CN$) δ 8.30 (d, 1H, $^3$J = 4.0 Hz), 8.22 (s, 1H), 7.85 (d, 1H, $^3$J = 7.6 Hz), 7.76 (s, 1H), 7.62 (dd, 1H, $^3$J = 7.2 Hz), 7.20 (dd, 1H, $^3$J = 6.8, $^3$J = 6.8 Hz), 1.33 (s, 9H); $^{13}$C-NMR (500 MHz, $CD_3CN$), δ155.2, 153.8, 153.3, 151.6, 138.5, 137.0, 130.6, 130.6, 130.0, 128.9, 127.5, 126.6, 126.4, 36.4, 31.8; MS (ESI) m/z (%): 1049.7 ($[Ag(C_{32}H_{30}N_4)_2]^+$, 14), 813.4 ($[Ag_2(C_{32}H_{30}N_4)_3]^{2+}$, 21), 618.4 ($[Ag(C_{32}H_{30}N_4)$ + MeCN$]^+$, 100), 578.2, ($[Ag_2(C_{32}H_{30}N_4)_2]^{2+}$, 18), 471.3 ($[(C_{32}H_{30}N_4)$+H$]^+$, 46), 455.2 ($[(C_{32}H_{30}N_4)$-Me+H$]^+$, 36%); UV - Vis ($CH_3CN$), $\lambda_{max}$ nm (log ε): 245 (5.1), 276 (4.9), 312 (4.6), 327 (4.5), 374 (4.6).

**$[Ag_2(2)_2][PF_6]_2$ (VII)**. A mixture of 2,5-di-*tert*-butyl-7,10-di(pyrimidin-2-yl)-8,9-diazafluoranthene (**2**) (0.03 g, 0.063 mmol) and $AgPF_6$ (0.016 g, 0.063 mmol) in $CD_3CN$ (2 mL) was stirred at RT overnight. $^1$H-NMR (400 MHz, $CD_3CN$) δ 8.60 (s, 1H), 8.59 (s, 1H), 8.39 (s, 1H), 8.17 (s, 1H), 7.39 (dd, 1H, $^3$J = 5.0, $^3$J = 5.0 Hz), 1.25 (s, 9H); $^{13}$C-NMR (500 MHz, $CD_2Cl_2$), δ 161.5, 158.9, 152.4, 152.3, 138.9, 130.3, 130.2, 129.6, 129.5, 128.6, 123.9, 36.0, 31.7; MS (ESI) m/z (%): 1053.8 ($[Ag(C_{30}H_{28}N_6)_2]^+$, 8), 816.8 ($[Ag_2(C_{30}H_{28}N_6)_3]^{2+}$, 6), 620.4 ($[Ag(C_{30}H_{28}N_6)$+ $CH_3CN]^+$, 21), 473.3 ($[(C_{30}H_{28}N_6)$ +H$]^+$, 100), 457.2 ($[(C_{30}H_{28}N_6)$-Me$]^+$, 21%); UV - Vis ($CH_2Cl_2$), $\lambda_{max}$ nm (log ε): 239 (5.0), 263 (4.8), 339 (4.7), 417 (4.6).

**$[Ag_2(2)_2][SbF_6]_2$ (VIII)**. A mixture of 2,5-di-*tert*-butyl-7,10-di-(pyrimidin-2-yl)-8,9-diazafluoranthene (**2**) (0.03 g, 0.063 mmol) and $AgSbF_6$ (0.022 g, 0.063 mmol) in acetone-$d_6$ (2 mL) was stirred at RT overnight. $^1$H-NMR (500 MHz, acetone-$d_6$) δ 8.93 (s, 2H), 8.68 (s, 1H), 8.35 (s, 1H), 7.65 (s, 1H), 1.31 (s, 9H); $^{13}$C-NMR (500 MHz, acetone-$d_6$), δ 160.9, 159.6, 153.0, 152.7, 139.5, 131.2, 130.8, 130.6, 130.1, 129.3, 124.5, 36.3, 31.9; MS (ESI) m/z (%): 1053.8 ($[Ag(C_{30}H_{28}N_6)_2]^+$, 8), 816.8 ($[Ag_2(C_{30}H_{28}N_6)_3]^{2+}$, 6), 620.4 ($[Ag(C_{30}H_{28}N_6)+CH_3CN]^+$, 21), 473.3 ($[C_{30}H_{28}N_6$+H$]^+$, 100), 457.2 ($[C_{30}H_{28}N_6$-Me$]^+$, 21%); UV - Vis ($CH_2Cl_2$), $\lambda_{max}$ nm (log ε): 239 (4.8), 263 (4.6), 339 (4.4), 419 (4.3).

**$[Ag_2(3)_2][PF_6]_2$ (IX)**. A mixture of 2,5-di-*tert*-butyl-7,10-di(thiazol-2yl)-8,9-diazafluoranthene (**3**) (0.01 g, 0.021 mmol) and $AgPF_6$ (0.005 g, 0.021 mmol) in $CD_3NO_2$ (1 mL) was stirred at RT overnight. $^1$H-NMR (500 MHz, $CDCl_3$) δ 9.82 (s, 1H), 8.03 (s, 1H), 8.01 (s, 1H), 7.59 (s, 1H) 1.30 (s, 9H), $^{13}$C-NMR (500 MHz, $CD_3NO_2$); δ 163.6, 155.0, 150.1, 146.0, 139.4, 131.9, 131.3, 130.7, 129.4, 128.8, 126.8, 37.0, 31.8; MS (ESI) m/z (%): 1073.5 $[Ag(C_{28}H_{26}N_4S_2)_2]^+$, 8), 632.3 ($[Ag(C_{28}H_{26}N_4S_2)+CH_3CN$+ H$]^+$, 100), 483.3 ($[C_{28}H_{26}N_4S_2$+H$]^+$, 18), 467.2 ($[C_{28}H_{26}N_4S_2$-Me+H$]^+$, 27%); UV - Vis ($CH_3CN$), $\lambda_{max}$ nm (log ε): 233 (5.0), 307 (4.8), 325 (4.9), 378 (4.6).

**$[Ag_2(3)_2][SbF_6]_2$ (X)**. A mixture of 2,5-di-*tert*-butyl-7,10-di(thiazol-2yl)-8,9-diazafluoranthene (**3**) (0.015 g, 0.031 mmol) and $AgSbF_6$ (0.011 g, 0.031 mmol) in $CD_3NO_2$ (1 mL) was stirred at RT overnight. $^1$H-NMR (500 MHz, $CDCl_3$) δ 9.90 (d, 1H, $^4$J = 1.2 Hz), 8.03 (d, 1H, $^3$J = 3.2 Hz), 7.99 (d, 1H, $^4$J = 1.6 Hz), 7.57 (d, 1H, $^3$J = 3.2 Hz), 1.32 (s, 9H), $^{13}$C-NMR (500 MHz, $CD_3NO_2$) δ 163.2, 155.0, 149.9, 145.9, 139.2, 131.9, 131.3, 130.7, 129.4, 128.8, 126.5, 37.0, 31.8; MS (ESI) m/z (%): 1073.5 ([Ag($C_{28}H_{26}N_4S_2$)$_2$]$^+$, 8), 632.3 ([Ag($C_{28}H_{26}N_4S_2$)+$CH_3CN$ +H]$^+$, 100), 483.3 ([$C_{28}H_{26}N_4S_2$+H]$^+$, 18), 467.2 ([$C_{28}H_{26}N_4S_2$-Me+H]$^+$, 27%); UV - Vis ($CH_3CN$), $\lambda_{max}$ nm (log ε): 233 (4.9), 307 (4.7), 325 (4.7), 378 (4.4).

## Crystal data

All X-ray crystal structure measurements were made on a *Nonius KappaCCD* area-detector diffractometer[18] or on an *Oxford Diffraction SuperNova Duo* diffractometer[19] using graphite monochromated Mo $K\alpha$ radiation ($\lambda$ = 0.71073 Å). All refinements were conducted on $F^2$ with SHELXL97;[20] H-atoms were included in geometrically calculated positions and allowed to ride on their parent atoms.

**2,5-Di-*tert*-butyl-7,10-di(pyridin-2-yl)-8,9-diazafluoranthene (1)**. Obtained from acetone, $C_{32}H_{30}N_4$, $M$ = 470.62, space group: $P\bar{1}$ (triclinic), $a$ = 10.2436(3), $b$ = 10.6985(2), $c$ = 12.3052(3) Å, $\alpha$ = 76.3104(14), $\beta$ = 81.3365(12), $\gamma$ = 76.8533(15)°, $V$ = 1269.20(5) Å$^3$, $Z$ = 2, $\mu$(Mo $K\alpha$) = 0.0733 mm$^{-1}$, $D_x$ = 1.231 g cm$^{-3}$, $2\theta_{(max)}$ = 55°, $T$ = 160 K, 37154 measured reflections, 5810 independent reflections, 4067 reflections with $I > 2\sigma(I)$, 332 parameters, $R(F)$ [$I > 2\sigma(I)$ reflections] = 0.0527, $wR(F^2)$ [all data] = 0.1450, goodness of fit = 1.033, $\Delta\rho_{max}$ = 0.25 e Å$^{-3}$.

**2,5-Di-*tert*-butyl-7,10-di(pyrimidin-2-yl)-8,9-diazafluoranthene (2)**. Obtained from dichloromethane/ pentane/benzene, $C_{30}H_{28}N_6$, $M$ = 472.59, space group: $P2_1$ (monoclinic), $a$ = 10.1555(2), $b$ = 12.3482(3), $c$ = 10.4107(2) Å, $\beta$ = 98.7439(14)°, $V$ = 1290.35(5) Å$^3$, $Z$ = 2, $\mu$(Mo $K\alpha$) = 0.0744 mm$^{-1}$, $D_x$ = 1.216 g cm$^{-3}$, $2\theta_{(max)}$ = 55°, $T$ = 160 K, 26745 measured reflections, 3094 independent reflections, 2843 reflections with $I > 2\sigma(I)$, 333 parameters, $R(F)$ [$I > 2\sigma(I)$ reflections] = 0.0375, $wR(F^2)$ [all data] = 0.0941, goodness of fit = 1.066, $\Delta\rho_{max}$ = 0.16 e Å$^{-3}$. The absolute structure was chosen arbitrarily.

**2,5-Di-*tert*-butyl-7,10-di(thiazol-2yl)-8,9-diazafluoran-thene (3)**. Obtained from acetonitrile/dichloro-methane/pentane, $C_{28}H_{26}N_4S_2$⊕$0.67CH_3CN$⊕$0.33C_5H_{12}$, $C_{31}H_{32}N_{4.67}S_2$, $M$ = 534.07, space group: $P42_1m$ (tetragonal), $a$ = 16.67987(11), $c$ = 15.01274(17) Å, V = 4176.82(6) Å$^3$, $Z$ = 6, $\mu$(Mo $K\alpha$) = 0.220 mm$^{-1}$, $D_x$ = 1.274 g cm$^{-3}$, $2\theta_{(max)}$ = 60°, $T$ = 160 K, 72287 measured reflections, 5846 independent reflections, 3959 reflections with $I > 2\sigma(I)$, 328 parameters, 343 restraints, $R(F)$ [$I > 2\sigma(I)$ reflections] = 0.0680, $wR(F^2)$ [all data] = 0.2199, goodness of fit = 1.088, $\Delta\rho_{max}$ = 0.57 e Å$^{-3}$. There are two symmetry-independent diazafluoranthene molecules in the structure. One of these molecules sits across a mirror plane which bisects the molecule. The other sits in a mirror plane as well as lying across a second mirror plane which bisects this molecule (mm symmetry). One *t*-butyl group in each molecule is disordered over two orientations and similarity restraints were employed in the refinement of these groups. The atomic displacement parameters suggest there might even be whole molecule disorder, but no attempt was made to develop such a model. There are voids in the structure, which appear to be partially occupied with solvent molecules. As attempts to model the solvent were unfruitful, the solvent contribution to the structure was removed using the *SQUEEZE* procedure of the program *PLATON*.[21] Full details are in the deposited CIF data.

**[$Cu_4(C_{30}H_{28}N_6)_4$][$PF_6$]$_4$⊕$2.17H_2O$ (I)**. Obtained from acetonitrile/methanol/acetone, $C_{120}H_{116.33}Cu_4F_{24}N_{24}O_{2.17}P_4$, $M$ = 2763.46, space group: $P\bar{1}$ (triclinic), $a$ = 12.4516(4), $b$ = 23.6077(8), $c$ = 42.950(2) Å, $\alpha$ = 99.3440(9), $\beta$ = 94.255(1), $\gamma$ = 94.401(1)°, V = 12372.9(7) Å$^3$, $Z$ = 4, $\mu$(Mo $Ka$) = 0.827 mm$^{-1}$, $D_x$ = 1.483 g cm$^{-3}$, $2\theta_{(max)}$ = 50°, $T$ = 160 K, 149307 measured reflections, 41319 independent reflections, 24116 reflections with $I > 2\sigma(I)$, 3551 parameters, 2062 restraints, $R(F)$ [$I > 2\sigma(I)$ reflections] = 0.0791, $wR(F^2)$ [all data] = 0.1762, goodness of fit = 1.077, $\Delta\rho_{max}$ = 0.81 e Å$^{-3}$. The asymmetric unit contains two tetranuclear cations, eight $PF_6^-$ anions, four sites fully occupied by what appear to be water molecules and one site approximately one-third occupied by a water molecule. Three *t*-butyl groups in one cation and one in the other are disordered. Some of the anions also show disorder and the disorder was modelled for two of the $PF_6^-$ anions. Similarity restraints were employed in the refinement of the disordered entities. Full details of the disorder treatment are in the deposited CIF data.

**[$Cu_4(C_{32}H_{30}N_4)_4$][$PF_6$]$_4$⊕$8C_3H_6O$ (II)**. Obtained from acetone/pentane, $C_{152}H_{168}Cu_4F_{24}N_{16}O_8P_4$, $M$ = 3181.11, space group: $Pbca$ (orthorhombic), $a$ = 23.9121(4), $b$ = 32.2190(4), $c$ = 38.8832(6) Å, V = 29956.6(8) Å$^3$, $Z$ = 8, $\mu$(Mo $K\alpha$) = 0.693 mm$^{-1}$, $D_x$ = 1.407 g cm$^{-3}$, $2\theta_{(max)}$ = 55°, $T$ = 160 K, 127500 measured reflections, 31301 independent reflections, 19963 reflections with $I > 2\sigma(I)$, 1760 parameters, 2788 restraints, R(F) [$I > 2\sigma(I)$ reflections] = 0.0874, $wR(F^2)$ [all data] = 0.2635, goodness of fit = 1.060, $\Delta\rho_{max}$ = 1.19 e Å$^{-3}$. The asymmetric unit contains one tetranuclear Cu-complex cation, four $PF_6^-$ anions and an estimated eight acetone molecules, some of which are highly disordered. Disorder was modeled for three of the eight unique *tert*-butyl groups in the cation. Some of the anions also show evidence of disorder and the disorder was modelled for one of the $PF_6^-$ anions. Similarity restraints were employed in the refinement of the disordered entities. As the disorder in many of the solvent molecules could not be modelled adequately, the solvent contribution to the diffraction data was removed using the SQUEEZE procedure of the program PLATON. Full details of the disorder and solvent treatment are in the deposited CIF data.

**[$Cu_4(C_{26}H_{25}N_4S_2)_4$][$PF_6$]$_4$⊕$2CHCl_3$⊕$2C_3H_6O$ (III)**. Obtained from chloroform/acetone/diethyl ether, $C_{120}H_{118}Cl_6Cu_4F_{24}N_{16}O_2P_4S_8$, $M$ = 3119.57, space group: $C2/c$ (monoclinic), $a$ = 14.8533(2), $b$ = 42.4657(4), $c$ = 23.1133(3) Å, $\beta$ = 95.2051(13)°, $V$ = 14518.7(3) Å$^3$, $Z$ = 4, $\mu$(Mo $K\alpha$) = 0.930 mm$^{-1}$, $D_x$ = 1.427 g cm$^{-3}$, $2\theta_{(max)}$ = 54.8°, $T$ = 160 K, 57097 measured reflections, 15081 independent reflections, 9224 reflections with $I > 2\sigma(I)$, 1120 parameters, 1518 restraints, $R(F)$ [$I > 2\sigma(I)$ reflections] = 0.0987, $wR(F^2)$ [all data] = 0.3243, goodness of fit = 1.161, $\Delta\rho_{max}$ = 1.48 e Å$^{-3}$. The asymmetric contains one half of a $C_2$-symmetric disordered tetranuclear Cu-complex cation, two $PF_6^-$ anions and one disordered molecule of each of chloroform and acetone. One of the two unique ligands in the cation is disordered over its entirety, while both *tert*-butyl groups of the other unique ligand are also disordered over two orientations. Similarity restraints were employed in the refinement of the disordered entities. The nature of the solvent molecules present was estimated from an assessment of the residual electron density peaks, although the indications are weak. The solvent molecules are disordered and clustered into two large cavities per unit cell, where each cavity contains four of each type of solvent molecule. As these solvent molecules could not be modelled sufficiently well, their contribution to the diffraction data was removed by using the *SQUEEZE* procedure of the program *PLATON*. Full details of the disorder treatment are in the deposited CIF data.

**[$Ag_2(C_{32}H_{30}N_4)_2$][$CHB_{11}Cl_{11}$]$_2$⊕$4C_6H_4Cl_2$⊕$CH_2Cl_2$ (IV)**. Obtained from acetonitrile/1,2-dichlorobenzene/hexane, $C_{91}H_{80}Ag_2B_{22}Cl_{32}N_8$, $M$ = 2873.74, space group: $P\bar{1}$ (triclinic), $a$ = 12.8147(2), $b$ = 14.1011(2), $c$ = 18.4969(2) Å, $\alpha$ = 75.5567(7), $\beta$ = 74.1397(7), $\gamma$ = 73.6649(7)°, $V$ = 3031.00(7) Å$^3$, $Z$ = 1, $\mu$(Mo $K\alpha$) = 1.074 mm$^{-1}$, $D_x$ = 1.574 g cm$^{-3}$, $2\theta_{(max)}$ = 60°, $T$ = 160 K, 88798 measured reflections, 17607 independent reflections, 13066 reflections with $I > 2\sigma(I)$, 620 parameters, $R(F)$ [$I > 2\sigma(I)$ reflections] = 0.0398, $wR(F^2)$ [all data] = 0.1053, goodness of fit = 1.059, $\Delta\rho_{max}$ = 0.53 e Å$^{-3}$. The asymmetric unit contains half of a centrosymmetric dinuclear cation, one anion, two molecules of 1,2-dichlorobenzene and a half occupied site for a molecule of

$CH_2Cl_2$, which is disordered about a centre of inversion. As a result of disorder, attempts to model one of the 1,2-dichlorobenzene molecules and the $CH_2Cl_2$ molecule were unsatisfactory, so the contribution of these solvent molecules to the structure was removed using the *SQUEEZE* procedure of the program *PLATON*. Full details are in the deposited CIF data.

**[Ag$_4$(C$_{32}$H$_{30}$N$_4$)$_4$][PF$_6$]$_4$⊕3C$_6$H$_6$⊕4MeCN (V)**. Obtained from acetonitrile/benzene/pentane, $C_{154}H_{150}Ag_4F_{24}N_{20}P_4$, $M$ = 3292.34, space group: $P\bar{1}$ (triclinic), $a$ = 13.9336(2), $b$ = 16.3976(2), $c$ = 19.5316(3) Å, $\alpha$ = 102.2393(6), $\beta$ = 106.5617(7), $\gamma$ = 112.3483(7)°, V = 3688.74(9) Å$^3$, $Z$ = 1, $\mu$(Mo $K\alpha$) = 0.654 mm$^{-1}$, $D_x$ = 1.482 g cm$^{-3}$, $2\theta_{(max)}$ = 60°, $T$ = 160 K, 100836 measured reflections, 21456 independent reflections, 14801 reflections with $I > 2\sigma(I)$, 1097 parameters, 816 restraints, $R(F)$ [$I > 2\sigma(I)$ reflections] = 0.0520, $wR(F^2)$ [all data] = 0.1328, goodness of fit = 1.022, $\Delta\rho_{max}$ = 1.33 e Å$^{-3}$. The asymmetric unit contains one half of the cationic Ag-complex, which lies across a centre of inversion, two $PF_6^-$ anions, two MeCN molecules, one disordered benzene molecule, which lies in a general position and one half of another benzene molecule, which lies across a centre of inversion. The *t*-butyl groups of the cation are all disordered over two orientations and similarity restraints were employed in the refinement of these groups. Full details of the disorder treatment are in the deposited CIF data.

**[Ag$_4$(C$_{32}$H$_{30}$N$_4$)$_4$][SbF$_6$]$_4$⊕4C$_5$H$_{12}$ (VI)**. Obtained from acetonitrile/acetone/benzene/pentane, $C_{148}H_{168}Ag_4F_{24}N_{16}Sb_4$, $M$ = 3545.30, space group: C2/$m$ (monoclinic), $a$ = 34.9940(6), $b$ = 17.4149(4), $c$ = 12.8469(3) Å, $\beta$ = 92.878(1)°, $V$ = 7819.2(3) Å$^3$, $Z$ = 2, $\mu$(Mo $K\alpha$) = 1.247 mm$^{-1}$, $D_x$ = 1.506 g cm$^{-3}$, $2\theta_{(max)}$ = 55°, $T$ = 160 K, 81452 measured reflections, 9187 independent reflections, 7602 reflections with $I > 2\sigma(I)$, 418 parameters, $R(F)$ [$I > 2\sigma(I)$ reflections] = 0.0399, $wR(F^2)$ [all data] = 0.0943, goodness of fit = 1.080, $\Delta\rho_{max}$ = 0.76 e Å$^{-3}$. The asymmetric unit contains one quarter of the cationic tetranuclear Ag-complex, which lies across a site of 2/$m$ symmetry ($C_{2h}$), two independent halves of $PF_6^-$ anions, which lie across mirror planes, and highly disordered solvent molecules, which are estimated to be pentane. As attempts to model the solvent were unfruitful, the solvent contribution to the structure was removed using the *SQUEEZE* procedure of the program *PLATON*. Full details are in the deposited CIF data.

**[Ag$_2$(C$_{30}$H$_{28}$N$_6$)$_2$][PF$_6$]$_2$⊕0.5CH$_2$Cl$_2$⊕0.5C$_6$H$_5$Cl⊕0.5C$_6$H$_{14}$ (VII)**. Obtained from dichloromethane/chlorobenzene/hexane/acetonitrile, $C_{66.5}H_{66.5}Ag_2F_{12}N_{12}P_2Cl_{1.5}$, $M$ = 1592.68, space group: $P2_1/c$ (monoclinic), $a$ = 17.7686(1), $b$ = 16.8498(2), $c$ = 23.2107(2) Å, $\beta$ = 90.2002(6)°, $V$ = 6949.2(1) Å$^3$, $Z$ = 4, $\mu$(Mo $K\alpha$) = 0.748 mm$^{-1}$, $D_x$ = 1.522 g cm$^{-3}$, $2\theta_{(max)}$ = 52°, $T$ = 160 K, 140014 measured reflections, 13650 independent reflections, 10805 reflections with $I > 2\sigma(I)$, 915 parameters, 234 restraints, $R(F)$ [$I > 2\sigma(I)$ reflections] = 0.0543, $wR(F^2)$ [all data] = 0.1623, goodness of fit = 1.074, $\Delta\rho_{max}$ = 1.01 e Å$^{-3}$. The asymmetric unit contains one cation, two disordered anions and some disordered solvent molecules which have been estimated at one half of each of a molecule of dichloromethane, chlorobenzene and hexane per asymmetric unit. As attempts to model the solvent were unfruitful, the solvent contribution to the structure was removed using the *SQUEEZE* procedure of the program *PLATON*. Similarity restraints were employed in the refinement of the disordered anions. Full details are in the deposited CIF data.

**[Ag$_2$(C$_{30}$H$_{28}$N$_6$)$_2$][SbF$_6$]$_2$⊕C$_3$H$_6$O⊕0.5C$_6$H$_{14}$⊕0.5C$_6$H$_6$ (VIII)**. Obtained from acetone/benzene/hexane, $C_{69}H_{72}Ag_2F_{12}N_{12}OSb_2$, $M$ = 1772.52, space group: C2/$m$ (monoclinic), $a$ = 23.2507(3), $b$ = 17.2660(3), $c$ = 17.6490(3) Å, $\beta$ = 91.746(1)°, $V$ = 7081.8(2) Å$^3$, $Z$ = 4, $\mu$(Mo $K\alpha$) = 1.380 mm$^{-1}$, $D_x$ = 1.662 g cm$^{-3}$, $2\theta_{(max)}$ = 55°, $T$ = 160 K, 75629 measured reflections, 8370 independent reflections, 7293 reflections with $I > 2\sigma(I)$, 472 parameters, 100 restraints, $R(F)$ [$I > 2\sigma(I)$ reflections] = 0.0456, $wR(F^2)$ [all data] = 0.1161, goodness of fit = 1.080, $\Delta\rho_{max}$ = 3.20 e Å$^{-3}$. The asymmetric unit contains half of a dinuclear cation, which sits across a mirror plane perpendicular to the Ag···Ag axis, two half anions, both of which sit on mirror planes and one of which is disordered, one half of a molecule of acetone, which also sits across a mirror plane and further highly disordered solvent molecules which have been estimated at one quarter of each of a molecule of hexane and benzene. As attempts to model the solvent were unfruitful, the solvent contribution to the structure was removed using the *SQUEEZE* procedure of the program *PLATON*. Similarity restraints were employed in the refinement of the disordered anion. Full details are in the deposited CIF data.

**[Ag$_2$(C$_{28}$H$_{26}$N$_4$S$_2$)$_2$]$_n$⊕2n[PF$_6$]$_n$⊕nC$_3$H$_6$O (IX)**. Obtained from acetonitrile/hexane/diethyl ether/acetone, $C_{59}H_{58}Ag_2F_{12}N_8OP_2S_4$, $M$ = 1529.06, space group: $P\bar{1}$ (triclinic), $a$ = 11.3226(2), $b$ = 11.5685(1), $c$ = 24.0375(4) Å, $\alpha$ = 101.105(1), $\beta$ = 100.426(2), $\gamma$ = 94.923(1)°, V = 3014.77(8) Å$^3$, $Z$ = 2, $\mu$(Mo $K\alpha$) = 0.926 mm$^{-1}$, $D_x$ = 1.684 g cm$^{-3}$, $2\theta_{(max)}$ = 59°, $T$ = 160 K, 53400 measured reflections, 14806 independent reflections, 13022 reflections with $I > 2\sigma(I)$, 894 parameters, 741 restraints, $R(F)$ [$I > 2\sigma(I)$ reflections] = 0.0967, $wR(F^2)$ [all data] = 0.2441, goodness of fit = 1.175, $\Delta\rho_{max}$ = 1.97 e Å$^{-3}$. The cation is a one-dimensional polymeric ribbon. The asymmetric unit contains two $Ag^+$ cations, two ligands, two $PF_6^-$ anions and one acetone molecule. One *tert*-butyl group in one of the independent ligands is disordered over two positions and the F-atoms of one of the independent $PF_6^-$ anions are also disordered over two positions. Similarity restraints were employed in the refinement of the disordered entities. The crystal was non-merohedrally twinned. The twin components are related by a rotation of 1.2° about the (001) plane with a major twin fraction of 0.806(2). Full details are in the deposited CIF data.

**Acknowledgment** SNF Project 200020_134998

**Electronic supplementary information (ESI) available**: crystallographic data in CIF format: CCDC 974463-974474.

## References

† Although footnotes will appear at the page bottom in the final printed article, for simplicity and ease of editing they should appear here during manuscript preparation and submission. These might include comments relevant to but not central to the matter under discussion, limited experimental and spectral data, and crystallographic data.


1 a) Chakrabarty, R.; Mukherjee, P. S.; Stang, P. *J. Chem. Rev.* 2011, **111**, 6810-6918; b) Leininger, S.; Olenyuk, B.; Stang, P. *J. Chem. Rev.* 2000, **100**, 853.

2 a) Lehn, J-M. Supramolecular Chemistry: Concepts and Perspectives; VCH: Weinheim 1995; b) Lehn, J-M. *Chem. Soc. Rev.* 2007, **36**, 151-160.

3 Steed, J. W.; Atwood, J. L. *Supramolecular Chemistry;* John Wiley: New York 2001.

4 a) Constable, E. C. *Tetrahedron*, 1992, **48**, 10013; b) Potts, K. T.; Keshavarz-K, M.; Tham, F. S.; Abruna, H. D.; Arana, C. *Inorg. Chem.* 1993, **32**, 4436.

5 a) Baxter, P. N. W.; Lehn, J-M.; De Cian, A.; Fischer, J. *Angew. Chem. Int. Ed.* 1993, **32**, 69; b) Fujita, M. Nagao, S.; Ogura, K. *J. Am. Chem. Soc.* 1995, **117**, 1649.

6 Sleiman, H.; Baxter, P. N. W.; Lehn, J-M.; Rissanen, K. *J. Chem. Soc. Chem. Commun.* 1995, 715.

7 Youinou, M.-T.; Rahmouni, N.; Fischer, J.; Osborn, J. *Angew. Chem. Int. Ed.* 1992, **31**, 133.

8 a) Ruben, M.; Rojo, J.; Romero-Salguero, F. J.; Uppadine, L. H.; Lehn, J-M. *Angew. Chem. Int. Ed.* 2004, **43**, 3644-3662; b) Baxter, P. N. W.; Lehn, J-M.; Fischer, J.; Youinou, M-T. *Angew. Chem. Int. Ed.* 1994, **33**, 2284; b) Stadler, A-M.; Burg, C.; Ramirez, J.; Lehn, J-M. *Chem. Commun.* 2013, **49**, 5733-5735.

9 a) Petty, M. C.; Bryce, M. R.; Bloor, D.; *Introduction to Molecular Electronics*, Oxford University Press, New York, 1995; b) Tour, J. M.; *Acc. Chem. Res.* 2000, **33**, 791-804; c) Pease, A. R.; Jeppesen, J. O.; Stoddart, J. F.; Luo, Y.; Collier, C. P.; Heath, J. R. *Acc. Chem. Res.* 2001, **34**, 433-444.

10 a) Joachim, C.; Gimzewski, J. K.; Aviram, A. *Nature* 2000, **408**, 541-548; b) Service, R. F. *Science* 2001, **293**, 782-785.

11 a) Chifotides, H. T.; Giles, I. D.; Dunbar, K. R. *J. A. Chem. Soc*. 2013, **135**, 3039-3055; b) Zheng, Y-Z.; Evangelisti, M.; Tuna, F.; Winpenny, R. E. P. *J. Am. Chem. Soc*. 2012, **134**, 1057-1065; c) Anwar, M. U.; Thompson, L. K.; Dawe, L. N.; Habib, F.; Murugesu, M. *Chem. Commun.* 2012, **48**, 4576-4578; d) Stefankiewicz, A. R.; Rogez, G.; Harrowfield, J.; Sobolev, A. N.; Madalan, A.; Huuskonen, J.; Rissanen, K.; Lehn, J-M. *Dalton Trans*. 2012, **41**, 13848-13855; e) Hutchinson, D. J.; Hanton, L. R.; Moratti, S. C. *Inorg. Chem*. 2011, **50**, 7637-7649; f) Carrion, M. C.; Ortiz, I. M.; Jalon, F. A.; Manzano, B. R. *Cryst. Growth. Des.* 2011, **11**, 1766-1776.

12 a) Rojo, J.; Romero-Salguero, F. J.; Lehn, J-M.; Baum, G.; Fenske, D. *Eur. J. Inorg. Chem.* 1999, 1421-1428; b) Patroniak, V.; Baxter, P. N. W.; Lehn, J-M.; Kubicki, M.; Nissinen, M.; Rissanen, K. *Eur. J. Inorg. Chem.* 2003, 4001-4009.

13 a) Zhao, L.; Xu, Z.; Thompson, L. K.; Heath, S. L.; Miller. D. O.; Ohba, M. *Angew. Chem. Int. Ed.* 2000, **39**, 3114-3117; b) Thompson, L.K.; Zhao, L.; Xu, Z.; Miller, D. O.; Reiff, W. M. *Inorg. Chem.* 2003, **42**, 128-139; c) Barbiou, M.; Lehn, J-M. *J. Am. Chem. Soc*. 2003, **125**, 10257-10265.

14 a) Zheng, Y-Z.; Evangelisti, M.; Tuna, F.; Winpenny, R. *J. Am. Chem. Soc*. 2012, **134**, 1057-1065; b) Ortiz, M. I.; Soriano, M. L.; Carranza, M. P.; Jalon, F. A.; Steed, J. W.; Mereiter, K.; Rodriguez, A. M.; Quinonero, D.; Deya, P. M.; Manzano, B. R. *Inorg. Chem.* 2010, **49**, 8828-8847; c) Dawe, L. N.; Abedin, T. S. M.; Thompson, L. K. *Dalton Trans.* 2008, 1661-1675; d) Moroz, Y. S.; Demeshko, S.; Haukka, M.; Mokhir, A.; Mitra, Utpal, M.; Stocker, M.; Muller, P.; Meyer, F.; Fritsky, I. O. *Inorg. Chem.* 2012, **51**, 7445-7447.

15 Rahanyan, N.; Linden, A.; Baldridge, K. K.; Siegel, J. S. *Org. Biomol. Chem.* 2009, **7**, 2082-2092.

16 Yang, L.; Powell, D. R.; Houser, R. P. *Dalton Trans*. 2007, 955-964.

17 a) Maekawa, M.; Miyazaki, T.; Sugimoto, K.; Okubo, T.; Kuroda-Sowa, T.; Munakata, M.; Kitagawa, S. *Dalton Trans*. 2013, **42**, 4258-4266; b) Constable, E. C.; Housecroft, C. E.; Neuburger, M.; Reymann, S.; Schaffner, S. *Cryst. Eng. Comm.* 2008, **10**, 991-995; c) Reymann, S. (2006). *New silver complexes with ligands based on 4-substituted-3,6-dipyridin-2-ylpyridazines*. Ph.D. Thesis. University of Basel, Switzerland; d) Schottel, B.; Chifotides, H. T.; Shatruk, M.; Chouai, A.; Perez, L. M.; Bacsa, J.; Dunbar, K. R. *J. Am. Chem. Soc.* 2006, **128**, 5895-5912. d) J. Klingele, S. Dechert and F. Meyer, *Coord. Chem. Rev*., 2009, **253**, 2698-2741. e) I. y. A. Gural'skiy, D. Escudero, A. Frontera, P. V. Solntsev, E. B. Rusanov, A. N. Chernega, H. Krautscheid and K. V. Domasevitch, *Dalton Trans*., 2009, 2856-2864. f) B. Happ, G. M. Pavlov, E. Altuntas, C. Friebe, M. D. Hager, A. Winter, H. Görls, W. Günther and U. S. Schubert, *Chem.– Asian J*., 2011, **6**, 873-880.

18 Hooft, R. *Kappa CCD Collect Software*, Nonius BV, Delft, The Netherlands, 1999.

19 *CrysAlisPro Diffractometer Software*, Oxford Diffraction Ltd, Yarnton, Oxfordshire, England, 2010.

20 Sheldrick, G. M. *Acta Cryst.* 2008, **A64**, 112.

21 a) Van der Sluis, P.; Spek, A. L. *Acta Cryst*. 1990, **A46**, 194-201; b) Spek, A. L. *PLATON*, *Program for the Analysis of Molecular Geometry*, University of Utrecht, The Netherlands, 2009.